TU/e EINDHOVEN UNIVERSITY OF TECHNOLOGY

Predictive modeling of the current density and radiative recombination in blue polymer-based light-emitting diodes

Citation for published version (APA):
Mensfoort, van, S. L. M., Billen, J. G. J. E., Carvelli, M., Vulto, S. I. E., Janssen, R. A. J., & Coehoorn, R. (2011). Predictive modeling of the current density and radiative recombination in blue polymer-based light-emitting diodes. *Journal of Applied Physics*, *109*(6), 064502-1/8. [064502]. https://doi.org/10.1063/1.3553412

DOI:
10.1063/1.3553412

Document status and date:
Published: 01/01/2011

Document Version:
Publisher's PDF, also known as Version of Record (includes final page, issue and volume numbers)

Please check the document version of this publication:

• A submitted manuscript is the version of the article upon submission and before peer-review. There can be important differences between the submitted version and the official published version of record. People interested in the research are advised to contact the author for the final version of the publication, or visit the DOI to the publisher's website.
• The final author version and the galley proof are versions of the publication after peer review.
• The final published version features the final layout of the paper including the volume, issue and page numbers.

Link to publication

General rights
Copyright and moral rights for the publications made accessible in the public portal are retained by the authors and/or other copyright owners and it is a condition of accessing publications that users recognise and abide by the legal requirements associated with these rights.

• Users may download and print one copy of any publication from the public portal for the purpose of private study or research.
• You may not further distribute the material or use it for any profit-making activity or commercial gain
• You may freely distribute the URL identifying the publication in the public portal.

If the publication is distributed under the terms of Article 25fa of the Dutch Copyright Act, indicated by the "Taverne" license above, please follow below link for the End User Agreement:

www.tue.nl/taverne

Take down policy
If you believe that this document breaches copyright please contact us at:

openaccess@tue.nl

providing details and we will investigate your claim.

Download date: 25. Aug. 2022

Predictive modeling of the current density and radiative recombination in blue polymer-based light-emitting diodes

S. L. M. van Mensfoort,[1,2,a)] J. Billen,[1,2] M. Carvelli,[1,2,3] S. I. E. Vulto,[2] R. A. J. Janssen,[1] and R. Coehoorn[1,2]

[1]*Molecular Materials and Nanosystems, Department of Applied Physics, Eindhoven University of Technology, P.O. Box 513, 5600 MB Eindhoven, The Netherlands*
[2]*Philips Research Laboratories, High Tech Campus 4, 5656 AE Eindhoven, The Netherlands*
[3]*Dutch Polymer Institute (DPI), P.O. Box 902, 5600 AX Eindhoven, The Netherlands*

(Received 15 October 2010; accepted 4 January 2011; published online 16 March 2011)

The results of a combined experimental and modeling study of charge transport, recombination and light emission in blue organic light-emitting diodes (OLEDs) based on a polyfluorene derivative are presented. It is shown that the measured temperature-dependent current-voltage curves and the voltage-dependent current efficiency are accurately described using an OLED device model that is based on the separately determined unipolar electron and hole mobility functions. The recombination rate is calculated using the Langevin formula, including recombination of holes with free as well as trapped electrons. The light emission is obtained from the exciton formation profile using independently determined values of the exciton radiative decay probability, the average dipole orientation, and assuming a fraction of singlet excitons $\eta_S = (22 \pm 3)\%$, close to the quantum-statistical value. No additional free parameter is used. This shows that predictive one-dimensional device modeling of OLEDs is feasible. © *2011 American Institute of Physics*. [doi:10.1063/1.3553412]

I. INTRODUCTION

The structurally disordered nature of the organic semiconductors used in organic light-emitting diodes (OLEDs) has a strong effect on the charge transport. Experimental[1] and theoretical[2–9] studies have made clear that the resulting energetic disorder of the states in between which the charge carrier hopping takes place does not only determine the temperature (T) and electric field (F) dependence of the mobility,[10] but that it also gives rise to a charge carrier density (n) dependence. Although various advanced numerical OLED device models have been developed and applied,[11–24] so far analyses of the current density and radiative recombination in full OLEDs, taking the carrier density dependence of the mobility into account, have not yet been reported. There is an urgent need for such an OLED device model, in order to make it possible to rationally design OLEDs with improved efficiency for applications such as large-area light sources.[25]

One of the issues which hampers the development of predictive OLED device models is that it has not yet been well established theoretically how the presence of disorder affects the electron-hole recombination rate. The recombination rate is usually assumed to be given by the Langevin formula $R = (e/\varepsilon)(\mu_h + \mu_e)n_h n_e$, with e the elementary charge, ε the electric permittivity, $\mu_{h(e)}$ the hole (electron) mobility and $n_{h(e)}$ the hole (electron) density.[26,27] Albrecht and Bässler studied recombination in the low-density (independent particle) Boltzmann limit using Monte Carlo (MC) calculations, and showed that at zero field the Langevin formula is then also applicable in the case of a disordered system with a Gaussian density of states (DOS).[28,29] A slight monotonically increasing enhancement of the recombination rate above the Langevin value was found with increasing field, in contrast to MC results obtained by Gartstein *et al.*,[30] who found a nonmonotonic field dependence of that enhancement ratio. Groves and Greenham found from MC calculations that considerable deviations from the Langevin formula, up to 40%, can occur.[31] In a recent MC study of the recombination rate, van der Holst *et al.* found similarly large deviations when applying (as in the work of Groves and Greenham) the Langevin formula using the unipolar electron and hole mobilities, i.e., the mobilities at the temperature, field and carrier density which are obtained from a MC calculation in the absence of carriers of the other polarity.[32] However, they discovered that the Langevin formula is well obeyed if bipolar mobilities are used, i.e., if the mobilities are used which follow from a MC calculation in the presence of carriers of the other polarity. The work focused on cases with equal electron and hole densities. So far, no expressions for the bipolar mobilities in cases of arbitrary density combinations are available. Within these publications also two possible additional complications were addressed, viz. the effect on the recombination rate of a mobility anisotropy[31] and the effect of correlation or anticorrelation between the electron and hole state energies on the same molecular site.[32] Finally, one might raise the question whether, in view of the disorder-induced filamentary of the current density in actual OLEDs,[33–38] the Langevin formula can still be applicable. One of the assumptions which leads to that formula is that the charge carrier transport occurs homogeneously across the device.

a)Author to whom correspondence should be addressed. Electronic mail: siebe.van.mensfoort@philips.com.

 © 2011 American Institute of Physics

Downloaded 27 May 2011 to 131.155.128.13. Redistribution subject to AIP license or copyright; see http://jap.aip.org/about/rights_and_permissions

In this paper, we demonstrate the feasibility of predictive modeling of the current density and recombination rate for the case of single layer OLEDs based on a blue-emitting copolymer. We show that the use of the standard Langevin formula for the bimolecular recombination rate is quite appropriate, in the sense that it leads to an accurate prediction of the voltage dependence of the current density and current efficiency. The light-emitting polymer (LEP, from the Lumation™ Blue Series, supplied by Sumation Co., Ltd.) studied consists of fluorene (PF) units copolymerized with (7.5 mol%) triarylamine (TAA) units, as shown in the inset of Fig. 1. For calculating the current density and the exciton-formation profile, we employ a recently developed one-dimensional drift-diffusion OLED device model.[39] The model is based on the experimentally determined (unipolar) hole[40] and electron[41] mobility functions. The recombination rate at zero field is described by the Langevin formula, whereas for finite fields an extension of that formula as described in Ref. 39 is used. Based on the results obtained in Refs. 40 and 41 the hole and electron densities of states are described as a Gaussian and as a Gaussian plus a superimposed exponential low-energy tail (representing deep trap states), respectively. The model includes in a parameter-free manner the recombination of holes with electrons occupying trap states. For calculating the current efficiency from the exciton formation profile, we employ an optical microcavity model (Lightex[42]) and use the values as obtained from independent experimental studies of the radiative decay probability of singlet excitons[43] and the average dipole angle.[44] The model leads to predicted current density (J) versus voltage (V) curves which are in excellent quantitative agreement with the experimental results. Furthermore, excellent agreement with the measured voltage dependent current efficiency is obtained assuming a singlet exciton formation probability equal to $\eta_S = (22 \pm 3)\%$, close to the quantum-statistical value of 1/4. The result is consistent with the range of values which was obtained recently by Carvelli *et al.* for the same polymer from an optical study of OLED devices.[45]

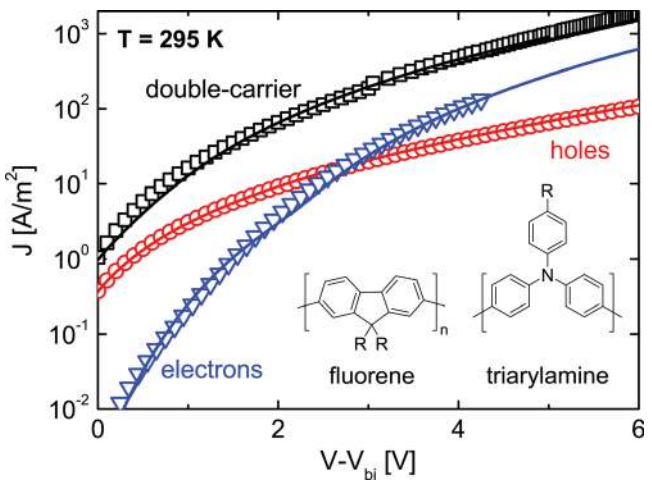

FIG. 1. (Color online) Measured $J(V)$ curves for a double-carrier OLED (squares; data obtained from pulsed measurements for $V - V_{bi} > 3$ V), a hole-only device (circles) and an electron-only device (triangles) with $L = 100$, 98, and 96 nm, respectively, at room temperature. The experimental data points have been corrected for a leakage current and a built-in voltage (V_{bi}, equal to 1.9, 1.0, and 3.0 V for the hole-only, electron-only, and double carrier devices, respectively). The solid curves are the result of the drift-diffusion modeling calculations. The inset shows the molecular structure of the PF-TAA copolymer studied.

The structure of the paper is as follows. In Sec. II, the device structure and experimental results are given. The modeling results are presented in Sec. III. Section IV contains a discussion, and the conclusions are given in Sec. V.

II. DEVICE STRUCTURE AND EXPERIMENTAL RESULTS

The double-carrier (DC) OLEDs studied are sandwich-type devices with the structure

glass | ITO | PEDOT:PSS | LEP | LiF | Ca | Al.

The devices were fabricated by spin coating a 100 nm poly(3,4-ethylenedioxythiophene):poly(styrene sulfonic acid) (PEDOT:PSS) layer on precleaned glass substrates covered with a 100 nm patterned indium tin oxide (ITO) layer in a nitrogen glovebox. Subsequently, the LEP layer was deposited by spin coating from a toluene solution, resulting in layer thicknesses L of 100 nm, as confirmed from measurements of the geometrical capacitance at low frequencies and low voltages. As a next step, thin layers of LiF (3 nm), Ca (5 nm), and Al (100 nm) were evaporated in high vacuum through a mask to form the top electrodes. To prevent the devices from water and oxygen contamination, the devices were encapsulated using a metal lid enclosing a desiccant getter. Twenty seven nominally identical 3×3 mm^2 devices were prepared on a single substrate.

Figure 1 shows the room temperature $J(V)$ curves for a hole-only (HO) diode (with a Pd cathode, see Ref. 40), an electron-only (EO) diode (with an AlO_x anode, see Ref. 41) and for a DC device, with a layer thickness $L = 98$, 96, and 100 nm, respectively (symbols). At high current densities, the $J(V)$ curve of the DC device was measured using a pulse method, in order to prevent from substantial heating. The $J(V)$ curves were corrected for a leakage current (see Ref. 40) and for a built-in voltage (V_{bi}) of 1.9, 1.0, and 3.0 V, respectively. The value of V_{bi} for the DC devices is determined from the voltage V_{peak} at which a peak in the low-frequency differential capacitance occurs (2.40±0.05 V), taking the same voltage difference between V_{peak} and V_{bi} as found for the hole-only devices into account (0.6 V).[40] Displaying the current densities as a function of $V - V_{bi}$ allows making a more proper comparison between the shapes of the $J(V)$ curves, as the devices have electrodes with different work functions. The HO and EO curves cross at a voltage $V - V_{bi} \approx 2.8$ V. Within a simplified picture of the charge transport, recombination and light outcoupling, the voltage at which the current densities in HO and EO devices are equal might be used to estimate the voltage at which in the DC device the hole and electron current densities are most optimally balanced, leading to an optimal light-outcoupling efficiency due to recombination taking place predominantly at relatively large distances from the quenching electrodes. It is already evident from Fig. 1 that this picture must actually be an oversimplification, as at the point where both curves

Downloaded 27 May 2011 to 131.155.128.13. Redistribution subject to AIP license or copyright; see http://jap.aip.org/about/rights_and_permissions

cross the double carrier current density is approximately one order of magnitude larger than the hole-only and electron-only current densities. Detailed device modeling will therefore be necessary to elucidate the interplay of the electron and hole current densities. Nevertheless, it is also shown that the double carrier devices indeed show a maximum current efficiency at approximately 3 V above the built-in voltage. It will be discussed how sensitive the current efficiency, its peak voltage and its peak value are to the detailed expressions assumed for the electron-hole recombination rate.

III. DEVICE MODELING

The solid curves in Fig. 1 are the result of single-carrier HO (Ref. 40) and EO (Ref. 41) device modeling using the extended Gaussian disorder model (EGDM). The densities of states assumed within these models are indicated in Fig. 2(a). The parameters describing the Gaussian hole (electron) DOS are the width $\sigma_{h(e)}$ and the density of transport sites $N_{t,h(e)}$. For electrons, the superimposed exponential trap DOS is described by a characteristic electron trap depth T_0 and a density of trap sites N_{trap}. The parameter values are given in the figure. The anode-polymer interface leads to a well-injecting contact (no injection barrier).[40] In Ref. 41 the injection barrier at the cathode-polymer interface (φ) was found to be 0.3 ± 0.1 eV. In this paper, a value $\varphi = 0.4$ eV has been used. Lowering of this barrier due to the image charge potential, as described in Ref. 46 is taken into account. The sensitivity of the results to the value of φ will be discussed in Sec. IV.

Figure 2(b) shows the temperature dependence of the hole (squares) and electron (circles) mobility in the limit of zero carrier density and zero electric field, μ_0. The parameter values given in Figs. 2(a) and 2(b) fully describe the hole (electron) transport in hole-only (electron-only) devices. The hole and electron transport are described by quite different parameter sets, as the hole transport takes place via the triarylamine monomeric units, whereas the electron transport takes place via PF-derived lowest unoccupied molecular orbital states.

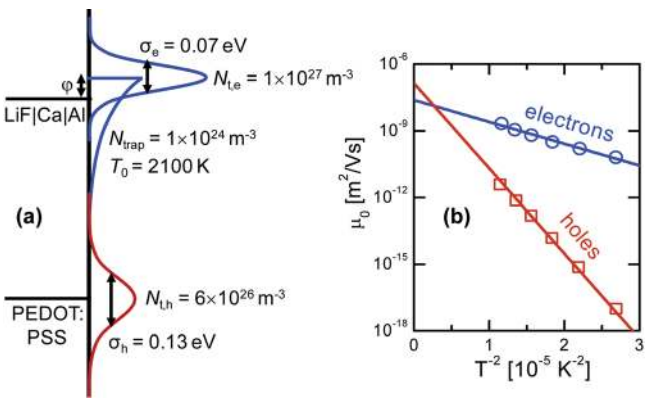

FIG. 2. (Color online) (a) Schematic representation of the energy level alignment in the devices studied, indicating the parameters and shape of the transport and trap DOS for electrons and hole transport, and the effective Fermi levels of the PEDOT:PSS and of the LiF | Ca | Al electrodes. (b) Temperature dependence of the electron and hole mobility in the zero field and zero carrier concentration limit (symbols), μ_0, in the Gaussian DOS. The solid curves are linear fits on this $\log(\mu_0)$ vs $1/T^2$ scale.

In the method used for solving the drift-diffusion-recombination problem for the DC devices,[39] the carrier densities and recombination rates across the thickness of the device are calculated on a discrete set of points on a one-dimensional grid, for the case of transport in a Gaussian DOS on which (for electrons) a trap DOS is superimposed. The one-dimensional Master-Equation (1D-ME) approach employed is mathematically different from the continuum device model[47] employed earlier in the HO and EO device studies. However, when applied to single-carrier devices, it is found to be essentially equivalent. Furthermore, in the 1D-ME model electron trapping is treated in the same manner as in the continuum EO model employed in Ref. 41 viz. by making use of the multiple-trap-and-release model.[48] Thermal equilibrium is assumed between charge carriers occupying host and trap states. The addition of deep trap states gives, at a given total density n_e, rise to a decrease of the Fermi energy, and hence to a decrease of the density of free" (mobile) charge carriers (charge carriers occupying the Gaussian host DOS). The local current density is only due to the drift and diffusion of these mobile carriers, with a density $n_{free} < n_e$. The trapped carrier density does not contribute in a direct manner to the current density. However, it affects the current density indirectly, as it contributes to the electrostatic field. This is calculated in a self-consistent manner from the total (free and trapped) carrier densities. Recombination is viewed as a local process, determined by the local carrier densities and field, and includes in a parameter-free manner the recombination due to hopping of free electrons to sites at which holes reside and due to hopping of holes to sites at which electrons (free *and* trapped) reside. At zero field, the local recombination rate is given by the Langevin-type expression

$$R = \frac{e}{\varepsilon}\left[n_{e,free} n_h \mu_e(n_{e,free}) + n_h n_e \mu_h(n_h)\right]. \quad (1)$$

The microscopic expression employed for modeling the recombination rate, from which Eq. (1) may be derived, is given in the Appendix. At finite fields, the recombination rate does not only increase as a result of the field-dependence of the mobilities, as expected from the Langevin formula, but it shows also an additional enhancement. As mentioned in the Introduction, such an effect was found by Albrecht and Bässler using three-dimensional Monte Carlo calculations.[29] The size of the effect as described by Eq. (A1) in the Appendix is close to that reported in Ref. 29 and can be explained by considering the three-dimensional nature of the recombination process.[39] Recombination is not only due to forward or backward hops but also to lateral hops which do not contribute to the mobility.

Figure 3(a) shows, for the 100 nm DC devices studied at $T = 293$, 253, and 213 K, a comparison between the experimental results (symbols) and the prediction as obtained from the drift-diffusion device model given in Ref. 39 (full curves), using the transport parameters as given in Fig. 2. The figure shows an excellent correspondence between model and experiment. In particular, it is indeed correctly

Downloaded 27 May 2011 to 131.155.128.13. Redistribution subject to AIP license or copyright; see http://jap.aip.org/about/rights_and_permissions

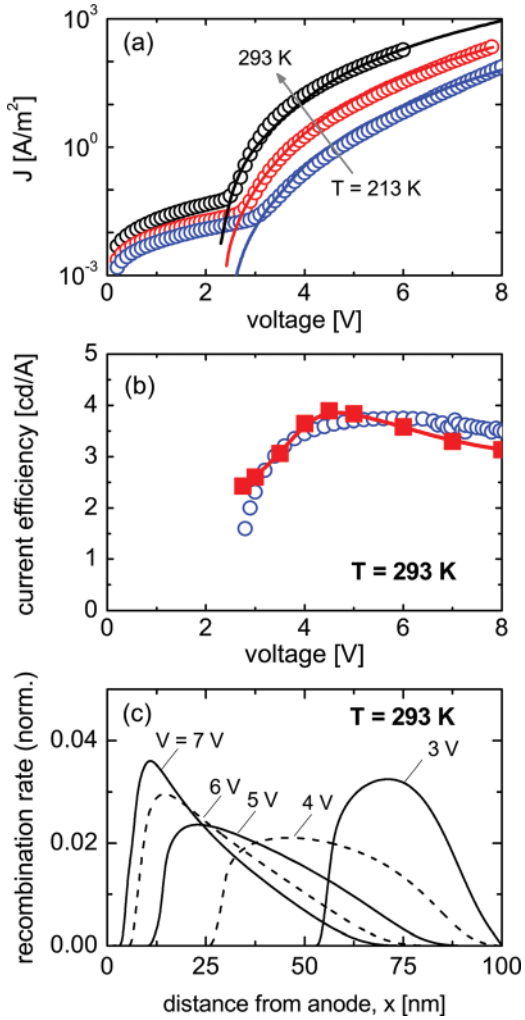

FIG. 3. (Color online) (a) Measured (open spheres) and calculated (solid curves) $J(V)$ curves for a double carrier device with $L = 100$ nm, at $T = 293$, 253, and 213 K; (b) measured (open spheres) and calculated (closed squares, connected by a solid curve) current efficiency as a function of the applied voltage at 293 K; and (c) calculated normalized recombination rate distributions at 293 K at various voltages.

predicted by the model that the double-carrier current density is in part of the voltage range almost one order of magnitude larger than either of the single-carrier current densities, such as observed close to the voltage at which the HO and EO $J(V)$ curves in Fig. 1 cross (at $V_{cross} = 5.8$ V, $\simeq$3 V above the built-in voltage).

Figure 3(b) (open spheres) shows that the measured voltage dependent current efficiency has a clear maximum at $\simeq$6 V, very close to V_{cross}. The current efficiency (in units cd/A) is here defined as the ratio of the luminance (in cd/m^2) measured perpendicular to the OLED surface and the current density (in A/m^2). The occurrence of a maximum may be understood from the calculated voltage dependence of the position (x)-dependent recombination rates $R(x)$ ("recombination profiles"), shown in Fig. 3(c) for $T = 293$ K. When the voltage increases from 3 V (transport "hole-dominated") to 7 V (transport "electron-dominated"), the peak in the recombination profiles shifts from a position more close to the cathode to a position close to the anode. It follows from the model that the recombination efficiency (fraction of charge carriers that contributes to exciton formation) is equal to 1 for $V \gtrsim 3$ V. The voltage dependence of the current efficiency is thus fully determined by the light-outcouping efficiency. This has been calculated using the optical microcavity outcoupling model Lightex,[42] including the effect of self-absorption in the PF-TAA layer in a manner as described in Ref. 44. Within the calculations, we use (i) the intrinsic source spectrum as obtained for PF-TAA in Ref. 44 (see Fig. 6(a) in that paper), (ii) the experimental PL quantum efficiency ($\sim 60\%$) (Ref. 43) as the radiative decay probability of the excitons in an infinitely thick medium, and (iii) a fully in-plane emitting dipole orientation, as expected from the predominantly in-plane orientation of the polymer chains after the use of the spin coating process and as confirmed from an analysis of emission experiments.[44] The real and imaginary refractive indices of all layers were determined using ellipsometry.[44]

The calculations reveal that the position at which the outcoupling efficiency is optimal is located at a distance of approximately 60 nm from the cathode. The steep rise of the current efficiency curve at $V = 2.5$ V can be rationalized by the notion that excitons that are close to the cathode have a high probability of transferring their energy nonradiatively to the electrode. This strongly reduces the light output at low voltages, when the recombination occurs relatively close to the cathode. With increasing voltage, the recombination profile shifts to a more central position in the device where the quenching due to the electrodes is strongly reduced so that the current efficiency increases. The fact that the current efficiency decreases then only slowly with increasing voltage can be understood from the fact that above 5 V the peak and shape of the recombination profiles do not change rapidly with voltage. We note that in the analysis of the current efficiency presented, a broadening or shift of the recombination profiles due to exciton diffusion has been neglected. The full curve in Fig. 3(b) shows the calculated current efficiency. The shape of the curve and the position of the maximum are in good agreement with the experimental data. A fraction of singlet excitons formed of 22% is assumed, in order to obtain an optimal quantitative correspondence.

IV. DISCUSSION

In the previous section, it was found that the voltage and temperature dependent double-carrier current density and the voltage dependence of the current efficiency measured at room temperature are in good agreement with the predictions based on earlier analyses of the single carrier mobilities, assuming (i) standard Langevin-recombination in the zero-field limit and a field-dependence of the rate as given in Ref. 39 (ii) recombination of holes with the free *and* the trapped electrons, and (iii) a fraction of singlet excitons formed of 22%, slightly smaller than the quantum-statistical value. In this section, we discuss several issues which might affect the accuracy of the analysis. We first focus on the modeling of the recombination process. Figures 4(a) and 4(b) show the voltage dependences of the current density and of the current efficiency, respectively, as calculated using various alternative model assumptions. Figure 4(c)

Downloaded 27 May 2011 to 131.155.128.13. Redistribution subject to AIP license or copyright; see http://jap.aip.org/about/rights_and_permissions

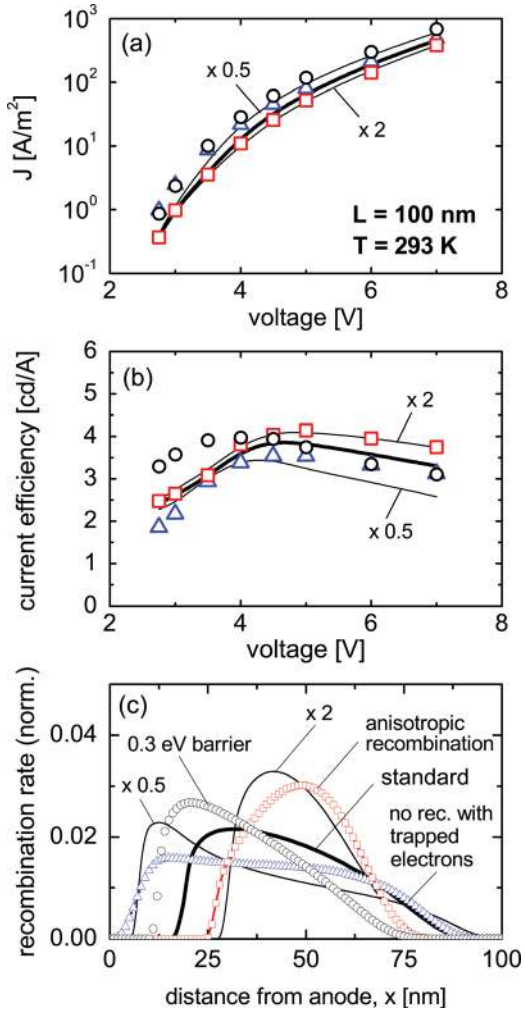

FIG. 4. (Color online) Effect of various alternative approaches for calculating the recombination rate on (a) the voltage dependence of the current density, (b) the voltage dependence of the current efficiency, and (c) the normalized recombination rate distribution, calculated at 4.5 V. All calculations were done for 100 nm devices at 293 K. The thick full curve gives the result as obtained using the Langevin formula assuming an isotropic mobility, including recombination with trapped electrons and assuming a 0.4 eV electron injection barrier. The thin full curves have been obtained using the same approach, assuming a recombination rate which is enhanced by a factor of 0.5 or 2, as indicated in the figures. The curves indicated by symbols give the results based on the same approach, but neglecting recombination with trapped electrons (triangles), assuming anisotropic recombination (squares) or assuming a 0.3 eV electron injection barrier (circles).

gives for all cases considered the normalized recombination profiles, calculated at 4.5 V. For reference purposes, curves (thin lines) are included which show the effect of taking a two times larger and two times smaller recombination rate as compared to the "standard" rate, given by Eq. (A1) in the Appendix. With increasing recombination rate, the current density becomes slightly smaller due to a reduction of the electron and hole carrier densities throughout the device. The effect is seen to be very small at small voltages, near the current density onset, and approximately 25% at 7 V. As expected, an increase of the recombination rate leads to a more narrow recombination profile, so that the peak current efficiency increases. The peak voltage of the current efficiency curve shifts slightly, from ≃4.5 to ≃5 V.

The standard approach used would overestimate the recombination rate when recombination with trapped electrons would actually be negligible. It is not *a priori* clear whether charge carriers that reside in trap states take part in the recombination process, although this has been proposed earlier. E.g., Burrows *et al*. argued that for the case of Alq_3-based OLEDs recombination between free holes and trapped electrons is even the predominant process,[49] and Blom *et al*. suggested that recombination of holes with trapped electrons could be a significant effect in PPV-based OLEDs.[19] In order to investigate this issue, we have carried out calculations within which only recombination with free electrons is included. As shown in Fig. 4(a) (blue triangles), the effect on the current density is only significant at small voltages, where the fraction of electrons occupying trap states is relatively large. Just as for the case of an overall reduction of the rate by a factor of 2, discussed above, the enhancement of the current density at small voltages can be explained as a consequence of the enhanced net space charge density in the device, resulting from the reduced recombination rate. Neglecting recombination with trapped electrons gives thus rise to a decreased steepness of the current-voltage curve, and thereby to worse agreement between the measured and modeled current densities. Due to the decreased recombination probability, the resulting recombination profiles are, for all voltages considered, significantly wider than as obtained when including recombination with trapped electrons. This may be seen from Fig. 4(c) for the case $V = 4.5$ V. As a result, the maximum of the current efficiency curve close to 4.5 V is approximately 8% lower.

On the other hand, the standard approach could also underestimate the recombination rate, viz. when the mobility in the in-plane direction is larger than the perpendicular mobility, which is the mobility employed in the Langevin equation. It is well-known that for the blue polymers investigated the spin-coating process leads strong optical anisotropy, resulting from a strong in-plane orientation of the polymer backbone which leads to a preference of the direction of the optical dipole moments within the layer plane.[44] Such an anisotropy can lead as well to a strong anisotropy of the mobility,[31] as is well-known for similar materials,[50] and to an enhancement of the effective recombination rate with respect to the Langevin rate when the field is oriented perpendicularly to the predominant chain direction.[51] For the PF-TAA polymers investigated, we only consider the electron mobility as (potentially) anisotropic. The electron transport is due to hopping in between PF-derived LUMO states, which might facilitate fast in-plane intrachain transport. In contrast, the hole transport is due to hopping between TAA-derived HOMO states. These are more localized, so that the interchain and intrachain mobilities are expected to be quite similar. We have investigated the possible effect of mobility anisotropy by performing calculations using a modified version of the formalism described in the Appendix, within which in the expression of the recombination rate given by Eq. (A1) the weight of the lateral hops is increased by a factor of four. In the limit of zero field, this would correspond to an increase of the total recombination rate by a factor of 3. The result on the current density, shown in Figs. 4(a)–4(c)

Downloaded 27 May 2011 to 131.155.128.13. Redistribution subject to AIP license or copyright; see http://jap.aip.org/about/rights_and_permissions

by red squares, is found to be for all voltages considered very similar to the result of calculations with an overall increase of the recombination rate with a factor of 2.

It may be concluded that the voltage dependences of the current-density are only weakly sensitive to the inclusion of recombination with trap states and to the inclusion of recombination anisotropy, although being able to predict the current density with an accuracy better than the observed $\pm 25\%$ differences might still be of practical importance. The current efficiency curves are already more sensitive, and the shapes of the emission profiles show the strongest sensitivity. Therefore, we view measurements of these profiles, using methods such as described in Ref. 44 as a necessary step toward the development of a refined model for the recombination process.

A different type of refinement of the recombination model would be the introduction in the Langevin formula of bipolar mobilities, instead of unipolar mobilities, as discussed in the Introduction. In the absence of a full theory of this effect, which should provide an expression for the ratio of the bipolar and unipolar mobilities in regions with unequal electron and hole densities, we cannot yet develop such an improved device model. However, it should be noted that the effect of the mutual interaction of carriers leading to a difference between the unipolar and bipolar mobilities is expected to be largest well within the recombination zone, were the electron and hole densities are similar, and that even in this zone the reduction of the rate is only typically a factor of 2.[32] Therefore, we envisage that the expected reduction of the current density will be rather limited. A more significant effect may be seen in the shape of the recombination profile. We expect that the spatial dependence of the bipolar mobility functions, due to the spatial dependence of the carrier densities, will give rise to a decrease of the width of the recombination zone.

The accuracy of the analysis given in the previous section is also affected by the experimental uncertainties in the parameters describing the electron and hole transport. Perhaps the largest and most relevant uncertainty concerns the electron injection barrier, taken to be equal to $\varphi = 0.4$ eV. This value is situated at the edge of the experimental uncertainty interval of 0.3 ± 0.1 eV given in Ref. 41. All other parameter values were taken to be equal to the value in the center of the uncertainty interval. The effect of taking $\varphi = 0.3$ eV is an increase of the current density by more than a factor 2 around the current density onset to approximately 70% at 7 V, as shown in Fig. 4(a) (black open circles). Furthermore, the enhanced electron density near the cathode and the resulting enhanced electron mobility give rise to a shift (at a fixed voltage) of the maximum in the recombination profile toward the anode. The calculated peak in the current efficiency curve decreases to approximately 4 V, and a strong increase of the predicted current efficiency at low voltages is obtained. All these results compare less favorably with experiment than the predictions obtained using $\varphi = 0.4$ eV. Therefore, we regard the latter value as more accurate.

We finally remark that some uncertainty might arise from the method used for including the effect of self-absorption in the emissive layer in the microcavity optical model.[44] If, alternatively, self-absorption is entirely neglected, and the source spectrum is taken to be equal to the (slightly more greenish) PL spectrum (see Fig. 6(a) of Ref. 44), we find a current efficiency which is approximately 15% larger than as shown in Fig. 3(b). The difference is quite independent of the voltage. This shows that even a drastic change in the treatment of self-absorption would only give rise to a small change of the singlet fraction obtained.

The uncertainties discussed above concerning the quantitative modeling of the transport, recombination and light-outcoupling processes do not give rise to a change of the overall picture: a steep predicted rise of the current efficiency, a maximum in the range 4–5 V, and a slow descent at higher voltages. Depending on the model assumptions, variations of the predicted maximum current efficiency of approximately $\pm 15\%$ are found, so that the assumed singlet fraction of 22% has an uncertainty of approximately $\pm 3\%$. This value is consistent with the independently determined value of $\eta_S = 17 \pm 7\%$ as obtained by Carvelli *et al.* from an analysis of the reverse bias photoluminescence (PL) and electroluminescence (EL) of PF-TAA based devices (but with a Ba/Al instead of a LiF/Ca/Al cathode).[45] Several studies have indicated that for organic semiconductor materials the EL singlet formation probability is close to 1/4, the quantum-statistical value.[52–55] However, it has been argued from other studies that it can be strongly enhanced, in particular in polymers.[56–64] For poly-phenylene-vinylene (PPV) based polymers, e.g., the singlet fraction as obtained using various methods ranges from approximately 20% (Ref. 52) to approximately 80% (Ref. 60). In view of this long-standing controversy, it is thus of interest that the value obtained by Carvelli *et al.* for PF-TAA, using an optical emission method, is found to be consistent with the value obtained in the present study, using device modeling.

V. SUMMARY AND CONCLUSIONS

In summary, it is shown for the first time that predictive modeling is possible for single-layer OLEDs. The model employed includes the effects of disorder and (EO) (Ref. 41) device modeling using the Extended Gaussian Disorder Model (EGDM), drift and diffusion of charge carriers, and recombination of holes with free and trapped electrons to form excitons. The voltage-dependent current efficiency, calculated from the voltage-dependent recombination profiles together with the position-dependent outcoupling efficiency, agrees well with experiment when a fraction of singlet excitons is assumed of $\eta_S = 22\%$. A discussion has been presented on the accuracy of this result, which is determined, firstly, by uncertainties concerning the appropriateness of the description of the recombination process assumed: (i) the role of recombination with trapped electrons, (ii) the possible role of mobility anisotropy and (iii) the effect of spatially disordered electron-hole interactions, leading to the recently introduced concept of a bipolar mobility. Secondly, the accuracy is determined by the uncertainties of the electron and hole transport parameters. It is shown that the shape of the emission profile is in general more sensitive to these issues than the current density, so that carrying out measurements

Downloaded 27 May 2011 to 131.155.128.13. Redistribution subject to AIP license or copyright; see http://jap.aip.org/about/rights_and_permissions

of that profile (using the experimental wavelength, angle and polarization dependent emission) would be recommended as a means to refine the modeling method employed. The resulting overall uncertainty in η_S is approximately 3%. The singlet fraction found is thus close to the value of 1/4 expected from quantum statistics, although slightly smaller. We believe that this finding contributes to solving the long-standing debate in the literature concerning the $S:T$ ratio.

ACKNOWLEDGMENTS

The authors would like to thank A. J. M. van den Biggelaar for skilful sample preparation, and Sumation Co., Ltd for the supply of Lumation™ Blue Series polymers. This research has received funding from the Dutch nanotechnology program NanoNed (contribution S.L.M.v.M.), and from the European Community's Program No. FP7-213708 (AEVIOM, contribution R.C.).

APPENDIX – MODELING OF THE RECOMBINATION RATE

Recombination at a site i is described as a local process, resulting from hops of holes (electrons) from nearest neighbor sites (with label j) to electrons (holes) at site i. It was shown in Ref. 39 that the three-dimensional nature of the recombination process is more properly taken into account if not only forward and backward hops are included (as in the calculation of the current density), but also four lateral hops from nearest neighbor (n.n.) sites in the plane which also includes site i (i.e., we have used the approach indicated as "$k=4$" in Fig. 3 of Ref. 39). The recombination rate is given by

$$R_{\mathrm{i}} = \frac{a'^2 e^2}{6\varepsilon k_{\mathrm{B}} T} \sum_{\text{n.n. sites}} \left(n_{\mathrm{e,free,j}} r_{\mathrm{e,ji}} n_{\mathrm{h,i}} + n_{\mathrm{h,j}} r_{\mathrm{h,ji}} n_{\mathrm{e,i}} \right), \qquad \text{(A1)}$$

with a' the distance between the grid points (close to the actual average intersite distance), k_{B} the Boltzmann constant, T the temperature, and r_{ji} the (local) carrier density and field dependent hop rates from sites j to i. The lateral hop rate is given by

$$r_{\mathrm{lat,i}} = \frac{\mu(n_{\mathrm{free,i}}, F=0) k_{\mathrm{B}} T}{a'^2 e}, \qquad \text{(A2)}$$

and the forward (backward) hop rates are given by

$$r_{\mathrm{ji}} = r_{\mathrm{lat,j}} \exp\left(\frac{\pm a' e F_{\mathrm{ij}}}{2 k_{\mathrm{B}} T} \right), \qquad \text{(A3)}$$

with $\mu(n_{\mathrm{free,i}}, F=0)$ the mobility corresponding to the hole or free electron density at site i at zero field and with F_{ij} the field in between sites i and j.[39] The proportionality constant in Eq. (A1) is taken such that at zero field and in the case of uniform electron and hole carrier densities the Langevin-type expression for the recombination rate given by Eq. (1) is obtained.

[1] C. Tanase, E. J. Meijer, P. W. M. Blom, and D. M. de Leeuw, Phys. Rev. Lett. **91**, 216601 (2003).
[2] M. C. J. M. Vissenberg and M. Matters, Phys. Rev. B **57**, 12964 (1998).
[3] S. D. Baranovskii, T. Faber, F. Hensel, and P. Thomas, J. Phys.: Condens. Matter **9**, 2699 (1997); S. D. Baranovskii, H. Cordes, F. Hensel, and G. Leising, Phys. Rev. B **62**, 7934 (2000); O. Rubel, S. D. Baranovskii, P. Thomas, and S. Yamasaki, *ibid.* **69**, 014206 (2004).
[4] V. I. Arkhipov, P. Heremans, E. V. Emelianova, G. J. Adriaenssens, and H. Bässler, J. Phys.: Condens. Matter **14**, 9899 (2002).
[5] Y. Roichman and N. Tessler, Synth. Met. **135–136**, 443 (2003); Y. Roichman, Y. Preezant, and N. Tessler, Phys. Status Solidi A **201**, 1246 (2004).
[6] W. F. Pasveer, J. Cottaar, C. Tanase, R. Coehoorn, P. A. Bobbert, P. W. M. Blom, D. M. de Leeuw, and M. A. J. Michels, Phys. Rev. Lett. **94**, 206601 (2005).
[7] R. Coehoorn, W. F. Pasveer, P. A. Bobbert, and M. A. J. Michels, Phys. Rev. B **72**, 155206 (2005).
[8] I. I. Fishchuk, V. I. Arkhipov, A. Kadashchuk, P. Heremans, and H. Bässler, Phys. Rev. B **76**, 045210 (2007).
[9] J. Zhou, Y. C. Zhou, J. M. Zhao, C. Q. Wu, X. M. Ding, and X. Y. Hou, Phys. Rev. B **75**, 153201 (2007).
[10] H. Bässler, Phys. Status Solidi B **175**, 15 (1993).
[11] P. W. M. Blom, M. J. M. de Jong, and S. Breedijk, Appl. Phys. Lett. **71**, 930 (1997).
[12] I. H. Campbell and D. L. Smith, *Solid State Physics: Advances in Research and Applications*, Vol. **55**, Academic Press, San Diego, pp. 1–117 (2001).
[13] P. S. Davids, A. S. Saxena, and D. L. Smith, J. Appl. Phys. **78**, 4244 (1996).
[14] B. K. Crone, P. S. Davids, I. H. Campbell, and D. L. Smith, J. Appl. Phys. **84**, 833 (1998).
[15] J. Shen and J. Yang, J. Appl. Phys. **83**, 7706 (1998).
[16] J. Staudigel, M. Stössel, F. Steuber, and J. Simmerer, J. Appl. Phys. **86**, 3895 (1999).
[17] G. G. Malliaras and J. C. Scott, J. Appl. Phys. **83**, 5399 (1998); G. G. Malliaras and J. C. Scott, *ibid.* **85**, 7426 (1999).
[18] J. C. Scott, P. J. Brock, J. R. Salam, S. Ramos, G. G. Malliaras, S. A. Carter, and L. Bozano, Synth. Met. **111**, 289 (2000).
[19] P. W. M. Blom and M. C. J. M. Vissenberg, Mater. Science and Engin. **27**, 53 (2000).
[20] W. Brütting, S. Berleb, and A. Mückl, Org. Electr. **2**, 1 (2001).
[21] A. B. Walker, A. Kambili, and S. J. Martin, J. Phys. Cond. Matter. **14**, 9825 (2002).
[22] B. Ruhstaller, T. Beierlein, H. Riel, S. Karg, J. Scott, and W. Riess, IEEE J. Sel. Topics Quantum Electr. **9**, 723 (2003).
[23] H. Houili, E. Tutiš, H. Lütjens, M. N. Bussac, and L. Zuppiroli, Comp. Phys. Comm. **156**, 108 (2003); D. Berner, H. Houili, W. Leo, and L. Zuppiroli, Phys. Status Solidi A **202**, 9 (2005).
[24] S. J. Konezny, D. L. Smith, M. E. Galvin, and L. J. Rothberg, J. Appl. Phys. **99**, 064509 (2006).
[25] B. W. D'Andrade and S. R. Forrest, Adv. Mater. **16**, 1585 (2004).
[26] P. Langevin, Ann. Chem. Phys. **28**, 433 (1903).
[27] M. Pope and C. E. Swenberg, *Electronic Processes in Organic Molecular Crystals* (Oxford University Press, New York, 1982).
[28] U. Albrecht and H. Bässler, Chem. Phys. Lett. **235**, 389 (1995).
[29] U. Albrecht and H. Bässler, Phys. Status Solidi B **191**, 455 (1995).
[30] Y. N. Gartstein, E. M. Conwell, and M. J. Rice, Chem. Phys. Lett. **249**, 451 (1996).
[31] C. Groves and N. C. Greenham, Phys. Rev. B **78**, 155205 (2008).
[32] J. J. M. van der Holst, F. W. A. van Oost, R. Coehoorn, and P. A. Bobbert, Phys. Rev. B **80**, 235202 (2009).
[33] Z. G. Yu, S. L. Smith, A. Saxena, R. L. Martin, and A. R. Bishop, Phys. Rev. B **63**, 085202 (2001).
[34] E. Tutiš, I. Batistic, and D. Berner, Phys. Rev. B **70**, 161202(R) (2004).
[35] K. D. Meisel, W. F. Pasveer, J. Cottaar, C. Tanase, R. Coehoorn, P. A. Bobbert, P. W. M. Blom, D. M. de Leeuw, and M. A. J. Michels, Phys. Status Solidi C **3**, 267 (2006).
[36] N. Rappaport, Y. Preezant, and N. Tessler, Phys. Rev. B **76**, 235323 (2007).
[37] J. J. Kwiatkowski, J. Nelson, H. Li, J. L. Bredas, W. Wenzel, and C. Lennartz, Phys. Chem. Chem. Phys. **10**, 1852 (2008).

Downloaded 27 May 2011 to 131.155.128.13. Redistribution subject to AIP license or copyright; see http://jap.aip.org/about/rights_and_permissions

[38]J. J. M. van der Holst, M. A. Uijttewaal, B. Ramachandhran, R. Coehoorn, P. A. Bobbert, G. A. de Wijs, and R. A. de Groot, Phys. Rev. B **79**, 085203 (2009).
[39]R. Coehoorn and S. L. M. van Mensfoort, Phys. Rev. B **80**, 085302 (2009).
[40]S. L. M. van Mensfoort, S. I. E. Vulto, R. A. J. Janssen, and R. Coehoorn, Phys. Rev. B **78**, 085208 (2008).
[41]S. L. M. van Mensfoort, J. Billen, S. I. E. Vulto, R. A. J. Janssen, and R. Coehoorn, Phys. Rev. B **80**, 033202 (2009).
[42]Lightex is a computer simulation tool, developed at Philips Research Aachen, for calculating the dipole-orientation dependent external emission spectrum as a function of the emitting dipole position in the cavity and as a function of the external emission angle and polarization.
[43]R. Coehoorn, S. Vulto, S. L. M. van Mensfoort, J. Billen, M. Bartyzel, H. Greiner, and R. Assent, Proc. SPIE **6192**, 61920O (2006).
[44]S. L. M. van Mensfoort, M. Carvelli, M. Megens, D. Wehenkel, M. Bartyzel, H. Greiner, R. A. J. Janssen, and R. Coehoorn, Nature Photonics **4**, 329 (2010).
[45]M. Carvelli, R. A. J. Janssen, and R. Coehoorn, Phys. Rev. B **83**, 075203 (2011).
[46]P. R. Emtage and J. J. O'Dwyer, Phys. Rev. Lett. **16**, 356 (1966).
[47]S. L. M. van Mensfoort and R. Coehoorn, Phys. Rev. B **78**, 085207 (2008).
[48]D. C. Hoesterey and G. M. Letson, J. Chem. Phys. Sol. **24**, 1609 (1963).
[49]P. E. Burrows, Z. Shen, V. Bulovic, D. M. McCarty, S. R. Forrest, J. A. Cronin, and M. E. Thompson, J. Appl. Phys. **79**, 7991 (1996).
[50]J. Zaumseil, R. J. Kline, and H. Sirringhaus, Appl. Phys. Lett. **92**, 073304 (2008).
[51]J. Zaumseil, Chr. Groves, J. M. Winfield, N. C. Greenham, and H. Sirringhaus, Adv. Funct. Mater. **18**, 3630 (2008).
[52]M. Segal, M. A. Baldo, R. J. Holmes, S. R. Forrest, and Z. G. Soos, Phys. Rev. B **68**, 075211 (2003).
[53]B. W. D'Andrade, M. A. Baldo, C. Adachi, J. Brooks, M. E. Thompson, and S. R. Forrest, Appl. Phys. Lett. **79**, 1045 (2001).
[54]M. A. Baldo, D. F. O'Brien, M. E. Thompson, and S. R. Forrest, Phys. Rev. B **60**, 14422 (1999).
[55]J. Zaumseil, Chr. R. McNeill, M. Bird, D. L. Smith, P. P. Ruden, M. Roberts, M. J. McKiernan, R. H. Friend, and H. Sirringhaus, J. Appl. Phys. **103**, 064517 (2008).
[56]Y. Cao, I. D. Parker, G. Yu, C. Zhang, and A. J. Heeger, Nature **397**, 414 (1999).
[57]J. S. Kim, P. K. H. Ho, N. C. Greenham, and R. H. Friend, J. Appl. Phys. **88**, 1073 (2000).
[58]M. Wohlgenannt, K. Tandon, S. Mazumdar, S. Ramasesha, and Z. V. Vardeny, Nature **409**, 494 (2001); M. Wohlgenannt, X. M. Jiang, Z. V. Vardeny, and R. A. J. Janssen, Phys. Rev. Lett. **88**, 197401 (2002).
[59]J. S. Wilson, A. S. Dhoot, A. J. A. B. Seeley, M. S. Khan, A. Köhler, and R. H. Friend, Nature **413**, 828 (2001).
[60]A. S. Dhoot, D. S. Ginger, D. Beljonne, Z. Shuai, and N. C. Greenham, Chem. Phys. Lett. **360**, 195 (2002).
[61]T. Virgili, G. Cerullo, L. Lüer, G. Lanzani, C. Gadremaier, and D. D. C. Bradley, Phys. Rev. Lett. **90**, 2474902 (2003).
[62]C. Rothe, S. M. King, and A. P. Monkman, Phys. Rev. Lett. **97**, 076602 (2006).
[63]K. Okumoto, H. Kanno, Y. Hamaa, H. Takahashi, and K. Shibata, App. Phys. Lett. **89**, 063504 (2006).
[64]A. P. Monkman, C. Rothe, and S. M. King, Proc. IEEE **97**, 1597 (2009).

Downloaded 27 May 2011 to 131.155.128.13. Redistribution subject to AIP license or copyright; see http://jap.aip.org/about/rights_and_permissions